Intra- and Interchain Correlations in Semidilute Polymer Solutions: Monte Carlo Simulations and Renormalization Group Results

M. Müller* and K. Binder

Institut für Physik, WA 331, Johannes Gutenberg Universität, D-55099 Mainz, Germany

L. Schäfer

Fachbereich Physik, Universität GH Essen D-45117 Essen, Germany

Received November 15, 1999; Revised Manuscript Received March 10, 2000

ABSTRACT: We investigate the intra- and intermolecular correlations in semidilute polymer solutions by large-scale computer simulations and renormalization group calculations. In the framework of the bond fluctuation model we study polymers with chain lengths up to $N = 2048$ monomers and determine the intermolecular pair correlation function, the coherent scattering intensity, and its distinct part at all length scales. The simulations are compared quantitatively to renormalization group calculations of the universal crossover scaling function. Special attention is paid to length scales smaller than the density screening length ξ, where the distinct part of the scattering function in the simulations is found to decay like $q^{-3-\alpha}$ with $\alpha = 0.7 \pm 0.2$. Various values of α ($0 \le \alpha \le 1$) have been predicted by scaling theories, RPA and P-RISM theories, and we discuss in detail a short distance type argument leading to $\alpha = 2/\nu + \omega_{12} - 3 \approx 0.8$, where ω_{12} denotes the ternary correction to scaling exponent. The scaling of the intermolecular pair correlation function on length scales larger than ξ is also investigated.

Introduction

The conformations of long flexible macromolecules in dilute and semidilute solutions have attracted long-standing interest.[1−4] An isolated self-repelling chain is swollen; its extension scales like $R \sim N^{\nu}$ with an exponent $\nu \approx 0.588$. The Flory exponent ν has been calculated by renormalization group techniques[1,2,4−6] and Monte Carlo simulations.[7] Upon increasing the monomer density ρ, the chains start to overlap and three regimes can be distinguished in the monomer pair correlation function: (a) On a local scale the packing of the monomers is determined by the detailed structure of the segments. (b) At intermediate distances, the probability of finding a monomer of the same chain is larger than that of a monomer of a different chain, and the chain statistics is that of a self-avoiding chain. (c) On larger length scales, the polymers interpenetrate and the pair correlation function is dominated by intermolecular contributions. The excluded volume interaction along a chain is screened, and the conformations on large length scales approximately obey Gaussian statistics. The length scale ξ at which the two behaviors (b) and (c) merge is the density screening length ξ. Beyond the local regime (a) the behavior of the chains is universal, i.e., independent of the monomeric structure. While the concentration and chain length dependence of single-chain properties have been explored in much detail, less is known about the spatial correlations among different molecules. The latter is important for understanding, e.g., the connectivity of networks cross-linked in semidilute solutions or the phase behavior in ternary mixtures of two polymers in a common solvent.[8] Finally, the largest length scale that matters is the size of the coil that now scales as $R \sim \xi^{1-1/2\nu} N^{1/2}$. Weak correlation effects extend up to this scale in semidilute solutions.

In very concentrated solutions or melts, the screening length ξ is microscopic and the single-chain autocorrelations are Gaussian down to the microscopic length scale b. The intermolecular pair correlation function $g^{\text{inter}}(\mathbf{r})$, which measures the probability of finding a monomer of a different molecule at a distance $\mathbf{r}$, is reduced. While the spatial extent of this correlation hole[9] increases with the chain's radius of gyration R_g, the number of contacts $z \sim \rho g^{\text{inter}}(b)$ between monomers of different chains converges for long chain lengths N toward a finite value with a $1/\sqrt{N}$ correction. The number of intermolecular contacts has attracted abiding interest, because it is related to the Flory−Huggins parameter in a binary blend.[10]

de Gennes[11] noted that correlation effects suppress contacts between different polymers in solutions compared to the melt. In dilute solutions scaling arguments suggest that the number of intermolecular contacts per monomer tends to zero in the long chain length limit. Renormalization group calculations[12−14] show that the number of intermolecular contacts per monomer also becomes very small in semidilute solutions of long chains. The number of intermolecular contacts is related to the effective Flory−Huggins parameter in a ternary blend of two polymers in a common solvent.[15] Ternary solutions have been investigated by Joanny, Leibler, and Ball[12] and by Schäfer and Kappeler.[13] More recently, the scaling of the number of contacts between two polymers (i.e., in the dilute limit) has been investigated,[16] and a relation between this scaling behavior and the short range behavior of the intermolecular pair correlation function in semidilute solutions has been suggested.[17]

The arrangement of polymers on length scales smaller than the density screening length has been studied by neutron scattering experiments,[18,19] analytical theory,[19−21] and computer simulations.[22] Unfortunately the different approaches did not yield mutually consistent results. In our investigation we revisit the problem of correlations on small length scales by Monte Carlo simulations in the framework of the bond fluctuation model.[23] Of course, by small length scales we here mean lengths

10.1021/ma991932u CCC: $19.00 © 2000 American Chemical Society
Published on Web 05/26/2000

much larger than b but still distinctly smaller than ξ, so universal behavior can be expected and a coarse-grained model is appropriate. Moreover, there are ongoing efforts to understand the inter- and intramolecular correlations in semidilute solutions both in a renormalization group framework and on the basis of the P-RISM theory. The Monte Carlo results might serve as a well-defined testing bed for these analytical theories.

Our paper is arranged as follows: In the next section we briefly summarize a phenomenological extension of the random phase approximation (RPA)[18,20,21] to semidilute solutions. These equations have been recently derived in the thread limit of the P−RISM theory[17] by treating the intermolecular excluded volume on a microscopic scale, and a renormalized form of RPA also emerges as the lowest order approximation of renormalized perturbation theory. Then we introduce the bond fluctuation model and define the quantities which we extract from the simulation. In the following section we give a brief account of the salient features of the renormalization group calculations, and we discuss the arguments which yield the large momentum behavior of the interchain correlation. The complicated full renormalization group results for the correlation functions are deferred to Appendices A and B. In the next section we discuss our Monte Carlo results on the properties of isolated chains and semidilute solutions and present a detailed quantitative comparison between the simulations and the renormalization group calculations. The paper closes with a discussion and a brief outlook.

II. Background

The single-chain properties and their scaling behavior on different length scales are experimentally accessible via the single-chain structure factor $S(\mathbf{q})$:

$$S(\mathbf{q}) = \frac{1}{N n_{\mathrm{poly}}} \sum_{\alpha=1}^{n_{\mathrm{poly}}} \langle |\sum_{i=1}^{N} \exp(i\mathbf{q}\mathbf{r}_{i\alpha})|^2 \rangle \qquad (2.1)$$

$S(\mathbf{q})$ is N times the customary form factor. The sum i runs over all N monomers of a polymer, while the index $\alpha = 1, ..., n_{\mathrm{poly}}$ labels the different polymers. $r_{i\alpha}$ denotes the position of monomer i of polymer α. In semidilute solutions different length scales correspond to distinct momentum dependencies:

$$S(\mathbf{q}) \sim \begin{cases} \text{nonuniversal} & q > 2\pi/b \\ q^{-1/\nu} & 2\pi/b \gg q \gg 2\pi/\xi \\ q^{-2} & 2\pi/\xi \gg q \gg 2\pi/R_{\mathrm{g}} \\ N(1 - q^2 R_{\mathrm{g}}^2/3) & 2\pi/R_{\mathrm{g}} \gg q > 0 \end{cases} \qquad (2.2)$$

where R_{g} denotes the radius of gyration, b is the characteristic length of the microscopic monomer structure, and ξ denotes the density screening length. In dilute solutions, $\xi \sim R_{\mathrm{g}}$ and then the third regime in eq 2.2 is absent. ξ is microscopic in melts,[9] which suppresses the second regime in eq 2.2. It needs semidilute solutions of very long chains in a good solvent to identify all four regimes. For such systems ξ is expected to scale with the segment density ρ as $\xi \sim \rho^{-\nu/(3\nu-1)}$.

In melts the RPA[18,20,21] yields a good description of the intra- and intermolecular correlations. Within this framework the coherent scattering intensity

$$G(\mathbf{q}) = \frac{1}{N n_{\mathrm{poly}}} \sum_{\alpha,\beta} \sum_{i,j=1}^{N} \langle \exp(i\mathbf{q}[\mathbf{r}_{i\alpha} - \mathbf{r}_{j\beta}]) \rangle \qquad (2.3)$$

takes the Ornstein−Zernike form:

$$G(\mathbf{q}) = \frac{S(\mathbf{q})}{1 + \nu\rho S(\mathbf{q})} \quad \text{or} \quad \frac{1}{G(\mathbf{q})} = \frac{1}{S(\mathbf{q})} + \nu\rho \qquad (2.4)$$

where ν parametrizes the strength of the pairwise monomeric interactions. While this might be appropriate also in concentrated solutions, it has been realized that it fails to incorporate the correlations of density fluctuations in the semidilute regime. Most notably the expression cannot describe the density dependence of the osmotic pressure $\Pi \sim \rho^{3\nu/(3\nu-1)}$, which is related to $G(\mathbf{q})$ via the compressibility sum rule

$$\frac{k_{\mathrm{B}}T}{G(\mathbf{q}\to 0)} = \frac{\partial \Pi}{\partial \rho} \qquad (2.5)$$

Nevertheless, data analysis in the semidilute regime is typically based on the RPA form (eq 2.4), where the violation of the sum rule is repaired in an *ad hoc* fashion by taking ν to be density dependent:

$$\nu \sim \rho^{[1/(3\nu-1)]-1} \qquad (2.6)$$

Recently, P-RISM theory[17] has been extended to semidilute solutions. This approach incorporates the intermolecular excluded volume on a microscopic level; the screening of the intramolecular interactions on length scales larger than ξ has been neglected. In the thread limit, the theory is analytically tractable and a density dependence of the effective interaction according to eq 2.6 has been derived. However, as will be discussed below, renormalization group calculations for $q \neq 0$ are not compatible with the simple replacement (eq 2.6).

Accepting the general structure of eq 2.4, we note that the term $\nu\rho$ plays an important role for the distinct part of the scattering function

$$H(\mathbf{q}) = \frac{1}{N n_{\mathrm{poly}}} \sum_{\alpha\neq\beta} \sum_{i,j=1}^{N} \langle \exp(i\mathbf{q}[\mathbf{r}_{i\alpha} - \mathbf{r}_{j\beta}]) \rangle = G(\mathbf{q}) - S(\mathbf{q}) \qquad (2.7)$$

Inserting the above RPA expression for the collective scattering function $G(\mathbf{q})$, one obtains

$$H(\mathbf{q}) = -\frac{\nu\rho S^2(\mathbf{q})}{1 + \nu\rho S(\mathbf{q})} \qquad (2.8)$$

If we employ a density-dependent pairwise interaction ν according to eq 2.6 and use the large q behavior of the single-chain structure factor, we find a scaling behavior of the form[17]

$$H(\mathbf{q}) \sim -(\rho\xi^3)(\xi q)^{-2/\nu} \sim (\xi q)^{-3.40} \qquad (2.9)$$

Of course, this expression does not describe the structure on the microscopic length scale. Therefore, this scaling behavior should be detectable in the range $2\pi/b > q > 2\pi/\xi$. Renormalization group results,[4] which will be described in more detail in section IV and in Appendix A, are in accord with a general RPA-type expression for $G(\mathbf{q})$, but replace $\nu\rho$ by a complicated function depending also on the momentum. A momentum dependence of $\nu\rho$ was foreseen already by Flory and

Bueche[24] and is also compatible with experiments and computer simulations.[22] It reflects correlations among different chains, which are built up in the range ξ. Such correlations are ignored in the simple mean field derivation of the standard RPA. Using the field theoretical short distance expansion, Jannink et al.[19] have derived the renormalization group prediction

$$H(\mathbf{q}) \sim \text{const}(\xi q)^{-d} + \text{const}\,(\xi q)^{-2/\nu-\omega} \qquad 1/b \gg q \gg 1/\xi \quad (2.10)$$

$$\sim \text{const}(\xi q)^{-3} + \text{const}(\xi q)^{-4.20} \quad \text{for} \quad d = 3$$

where $\omega \approx 0.80$ ($d = 3$) is the standard correction to scaling exponent. As has been pointed out in ref 4, section 19.4, however, one might suspect that the subleading term should be replaced by $(\xi q)^{2/\nu-\omega_{12}}$, where $\omega_{12} \approx 0.40$ ($d = 3$)[14] is the correction to scaling exponent in a ternary polymer solution. It, for instance, governs the scaling of the number of contacts σ_2 of two mutually interpenetrating chains, $\sigma_2 \sim N^{-\nu\omega_{12}}$, as well as the scaling of the ternary Flory−Huggins parameter χ in a semidilute solution, $\chi \sim \rho^{(1+\nu\omega_{12})/(3\nu+1)}$. Indeed, in recent work[17] the form

$$H(\mathbf{q}) \sim (\xi q)^{-2/\nu-\omega_{12}} \approx (\xi q)^{-3.80} \qquad (2.11)$$

has been suggested. We discuss the argument leading to eq 2.11 and its relation to field theoretic work in more detail in section IV and Appendix B.

A power-law dependence on momentum corresponds to a characteristic power law in the spatial dependence of the corresponding pair correlation function. The intermolecular pair correlation function

$$\rho g^{\text{inter}}(\mathbf{r}) = \frac{1}{N n_{\text{poly}}} \sum_{\alpha \neq \beta} \sum_{i,j=1}^{N} \langle \delta(\mathbf{r}_{i\alpha} - \mathbf{r}_{j\beta} - \mathbf{r}) \rangle \qquad (2.12)$$

is related to the distinct part of the coherent scattering function $H(\mathbf{q})$ via

$$\rho g^{\text{inter}}(\mathbf{r}) = \int \mathrm{d}^3 q \, \exp(-i\mathbf{q}\mathbf{r}) \, H(\mathbf{q}) \qquad (2.13)$$

Since the accessible momentum range on which the characteristics of the intermolecular arrangement in semidilute solutions dominate is rather small, it is also worth exploring the spatial dependence of the pair correlation functions. Equations 2.9 or 2.11 yields the small distance behavior $g^{\text{inter}}(r) \sim r^{3-2/\nu}$ or $g^{\text{inter}}(r) \sim r^{3-2/\nu-\omega_{12}}$, respectively, while eq 2.10 suggests a logarithmic behavior, $g^{\text{inter}}(r) \sim \ln r$.

The distinct part of the scattering intensity is not easily accessible, and there are only a few experimental studies. In experiments both the single-chain structure factor and the coherent structure factor have to be measured in absolute units. Their difference results in $H(\mathbf{q})$, which is much smaller than the individual contributions in the q regime of interest. Moreover, a clear separation of length scales is also not always obtained in experiments, and the effects of polydispersity have to be taken into account. Ullman et al.[18] found fair agreement between the scattering data for polystyrene in toluene and the RPA expressions. They did find evidence for a concentration dependence of the monomeric interaction v. Moreover, the authors note that v also exhibits a small q dependence. Experiments by Jannink and co-workers[19] found deviations from the RPA compatible with a dependence of the form $H(\mathbf{q}) \sim q^{-3}$. However, under the experimental conditions the screening length exceeded the statistical segment length only by a factor of 2.5. The intermolecular arrangement in polymer solutions also determines the miscibility behavior of two polymers in a common solvent. The Flory−Huggins parameter χ scales in the same way as the contact value of the intermolecular pair correlation function. Experiments[8] do find evidence for a renormalization of the Flory−Huggins parameter by a factor of $\rho^{(1+\nu\omega_{12})/(3\nu-1)}$ as predicted by Joanny, Leibler, and Ball[12] and by Schäfer and Kappeler.[13,14]

Investigations of the intermolecular arrangement in semidilute solutions via Monte Carlo simulations are rare. A Monte Carlo simulation by Sariban and Binder[25] investigated the scaling of the critical temperature in a ternary solution with density and chain length for short chain length $N \leq 64$. The data are compatible with the predicted renormalization of the Flory−Huggins parameter. A recent Monte Carlo simulation by Yamakov et al.[22] investigated the spatial dependence of the intermolecular arrangement for chain length $N \leq 256$. Though the study found deviations from the RPA prediction, e.g., a momentum dependence of the effective interaction parameter v, they could not confirm the prediction of Jannink et al.[19] Straightforward fitting of the raw data for the distinct part of the structure factor yields a dependence of the form $H(\mathbf{q}) \approx q^{-3.67}$ not far from the prediction of eq 2.11 quoted above. However, it is not clear whether the appropriate regime of intermediate length scales has been truly reached. In any case, the conclusion about the previous work is that the problem seems unresolved, and different approaches yielded contradictory results.

III. Model and Monte Carlo Technique

Monte Carlo (MC) simulations might contribute to the investigation of the controversial predictions, because the distinct part of the coherent scattering function is directly accessible. However, to observe the predicted power-law behavior of the semidilute regime, the conditions $b \ll \xi \ll R_g$ must be met to achieve a separation of length scales. Ideally, the microscopic length scale and the radius of gyration should differ by at least 2 orders of magnitude, and hence, one needs chain lengths on the order of 10^3-10^4. The generation of independent configurations of multichain systems of such long chains poses computational difficulties. A recent study of Yamakov et al.[22] addressed the questions by MC simulations of an off-lattice model with local updates of the chain conformations. However, their study was restricted to chain lengths $N \leq 256$ monomers, which prevented full compliance with the above double inequality.

Lattice models have proven useful in understanding the universal properties of polymeric systems. In the present work we use the bond-fluctuation model.[23] In the framework of this model a single monomer occupies all eight corners of a single cubic lattice, preventing these sites from further occupancy. Monomers along a polymer are connected via one of 108 bond vectors of lengths 2, $\sqrt{5}$, $\sqrt{6}$, 3, and $\sqrt{10}$. All lengths are measured in units of the lattice constant. The bonding vectors are chosen such that bonds do not cross each other during the local hopping of monomers. This model combines the computational efficiency of lattice models with a rather faithful representation of continuous space prop-

erties. Using a local hopping algorithm, Paul et al.[26] explored the static and dynamic single-chain properties from the isolated chain up to meltlike densities. However, only chains with lengths up to $N = 200$ monomers have been considered. The osmotic pressure as a function of density and chain length[27] and the intermolecular pair correlation function at meltlike densities[28] have also been studied for this model.

In the present work we employ a slithering snake algorithm[28,29] to update the chain conformations on the lattice. A monomer is added to a randomly chosen chain end, and the monomer at the opposite end of the polymer is removed. Each accepted move displaces the center of mass of a chain by an amount on the order of N^{ν}/N. Hence, this algorithm relaxes the large-scale conformations of the polymers a factor $N^{2\nu}$ faster than a local update of individual monomer positions. This permits us to study chains up to $N = 2048$ monomers at semidilute densities. In principle, more sophisticated algorithms could be envisaged (e.g., pivot,[30] configurational bias,[31] or recoil growth[32]). However, their efficiency depends rather sensitively on density and chain length.

The two systems simulated consist of $n_{\mathrm{poly}} = 100$ polymers of length $N = 2048$ in a cubic simulation cell of sizes $L = 256$ and $L = 400$. This corresponds to monomer number densities $\rho = 0.0122$ and 0.0032. Every 500 000 slithering snake attempts per chain a configuration was stored for further analysis. The acceptance ratio of the moves at this density is 0.676 for $L = 256$ and 0.772 for $L = 400$. We generated 836 and 2550 configurations for the $L = 256$ and the $L = 400$ box sizes, respectively. The system size is limited by the computer memory; the largest grid requires about 500 MB of memory. In addition, we have performed single-chain simulations to investigate the intramolecular correlations (in dilute solutions) and to determine from which length scale onward the asymptotic behavior of self-avoiding chains is observed. For $N \leq 1024$ we used $L = 256$, while for $N = 2048$ and 4096 we have employed $L = 400$. For $N = 4096$ systematic deviations from the behavior of an isolated chain have to be expected, because the chain extension is comparable to the system size L.

IV. Renormalization Group Theory

Both the intramolecular and the total structure factors can be calculated by renormalized perturbation theory, and the results of a first-order ("one-loop") calculation covering all the crossover from dilute to semidilute systems also outside the asymptotic excluded volume limit are available.[4] The detailed expressions are complicated and are collected in Appendix A. Here, we only sketch some basic features of the theory.

The renormalized theory is a sophisticated version of the standard two-parameter theory,[33] constructed such that the limit of long chains $N \to \infty$ can be taken. The two parameters are contained in the basic variables

$$\tilde{z} = \tilde{v}\sqrt{N} \quad \text{and} \quad \tilde{R}_0{}^2 = \tilde{l}^2 N \tag{4.1}$$

where $\tilde{z}$ replaces the interaction parameter z of the naive two-parameter theory and $\tilde{R}_0{}^2$ is the radius of gyration of a fictitious noninteracting chain. (Note that in all this discussion we restrict ourselves to the physical dimension $d = 3$. For general d, $\tilde{z}$ takes the form $\tilde{z} = \tilde{v}N^{2-d/2}$.) The two parameters $\tilde{v}$ and $\tilde{l}$ depend on the microstructure of the chain and on the temperature, but they are independent of chain length and concentration. The concentration is measured in terms of an overlap variable

$$\tilde{s} = c_{\mathrm{p}}\tilde{R}_0{}^3 \tag{4.2}$$

where $c_{\mathrm{p}} = \rho/N$ is the number density of chains.

In the renormalization group (RG) theory one proves that the physical observables obey "nonlinear scaling laws". An important example is the law for the radius of gyration in a solution of finite concentration

$$R_{\mathrm{g}}{}^2 = \tilde{R}_0{}^2 \tilde{R}_{\mathrm{g}}(\tilde{s},\tilde{z}) \tag{4.3}$$

The "scaling function" $\tilde{R}_{\mathrm{g}}$ in the dilute limit $\tilde{s} = 0$ reduces to the theoretical swelling factor

$$R_{\mathrm{g}}{}^2/\tilde{R}_0{}^2|_{\tilde{s}=0} = \tilde{R}_{\mathrm{g}}(0,\tilde{z}) = \tilde{\alpha}_{\mathrm{g}}{}^2(\tilde{z}) \tag{4.4}$$

The single-chain structure factor and the coherent scattering intensity obey the scaling laws

$$(1/N)S(\mathbf{q}) = J_{\mathrm{a}}(q^2\tilde{R}_0{}^2,\tilde{s},\tilde{z})$$
$$(1/N)G(\mathbf{q}) = J_{\mathrm{c}}(q^2\tilde{R}_0{}^2,\tilde{s},\tilde{z}) \tag{4.5}$$

In principle, all the scaling functions also depend on the chain length distribution in the solution, a dependence suppressed here since we only are concerned with monodisperse systems. The scaling functions are universal, and the scaling laws are strictly valid in the limit $N \to \infty$, $\rho = c_{\mathrm{p}}N \to 0$, and $q^2\tilde{l}^2 \to 0$. The scaling variables $\tilde{z}$, $\tilde{s}$, and $q^2\tilde{R}_0{}^2$ may take any value; however $0 \leq \tilde{z}$, $\tilde{s}$, $q^2\tilde{R}_0{}^2 < \infty$.

The scaling functions can be calculated perturbatively within the framework of the loop expansion. This expansion proceeds in powers of a "renormalized coupling" u, which in some sense measures the interaction among whole strands of the chains. It is a "running" coupling, which means that it depends on the length scale l_{R} considered. For $l_{\mathrm{R}} \to \infty$ it reaches a fixed point u^*. This is known as the "excluded volume limit", where the nonlinear scaling laws reduce to power-law scaling as employed in section II. More specifically, the parameter $\tilde{z}$ tends to infinity and scaling functions like $J_{\mathrm{a,c}}$ reduce to functions of only two variables:

$$(1/N)S(\mathbf{q}) = J_{\mathrm{a}}{}^*(q^2R_{\mathrm{g}}{}^2(0),s) \tag{4.6}$$

$$(1/N)G(\mathbf{q}) = J_{\mathrm{c}}{}^*(q^2R_{\mathrm{g}}{}^2(0),s) \tag{4.7}$$

Here $R_{\mathrm{g}}{}^2(0)$ is the radius of gyration of an isolated chain, and s is the "geometrical overlap" defined as

$$s = c_{\mathrm{p}}R_{\mathrm{g}}{}^3(0) \tag{4.8}$$

Similarly, the scaling law (eq 4.3) reduces to $R_{\mathrm{g}}{}^2 = R_{\mathrm{g}}{}^2(0)\, R^*(s)$.

Turning again to the general situation where u may differ from u^*, we note that the length scale l_{R} in the evaluation of the theory has to be chosen to be on the order of the smallest macroscopic length of interest. This imposes a crossover condition of the form

$$l_{\mathrm{R}}{}^{-2} \sim q^2 + \mathrm{const}/\xi_{\mathrm{d}}{}^2 \tag{4.9}$$

where

$$\xi_d^{\,2} = -(1/2)\Delta_{q\to 0} \ln G(\mathbf{q}) \qquad (4.10)$$

is the density correlation length in the system.[34] This condition incorporates the ideas of the concentration blob model[9] and screening into the theory: For $q^2 \ll \xi_d^{-2}$ the system is represented as a solution of weakly interacting blobs of size ξ_d, $l_R \sim \xi_d$. For $q^2 \gg \xi_d^{-2}$ we are looking deep inside a blob, and the scale is set by $l_R \approx 1/q$. As a result the running coupling becomes a function of the scaling variables.

$$u/u^* = f = f(\tilde{s},\tilde{z},q^2\tilde{R}_0^{\,2}) \qquad (4.11)$$

For further explanations of the renormalized theory we refer to the literature.[4] The explicit form of the RG mapping used here is given in Appendix A.

We now turn to the perturbative calculation of the scaling functions. The lowest order ("zero-loop") approximation yields the renormalized form of RPA. In the excluded volume limit $u \to u^*$, i.e., $f \to 1$, it reduces to the expressions of section II, except that the coupling v must be replaced by a quantity depending on both $q^2R_g^{\,2}(0)$ and the geometrical overlap variable s.

The one-loop correction for the scaling functions J_a and J_c (cf. eqs 4.5) shows an interesting new effect. For semidilute systems the small q expansion develops a term of the type $(q^2\xi_d^{\,2})^{3/2}$. For example, the intramolecular structure factor at the fixed point $u = u^*$ takes the form

$$s^{-1/(3\nu-1)} J_a^{\,-1}(\mathbf{q}) = a_1 q^2\xi_d^{\,2} + a_2(q^2\xi_d^{\,2})^{3/2} + O(q^4\xi_d^{\,4}) \quad \text{for} \quad s \to \infty \qquad (4.12)$$

where a_1 and a_2 are universal positive numbers. This implies that J_a^{-1} as a function of $q^2\xi_d^2$ develops a singular curvature for $q^2\xi_d^2 \to 0$, a result also found for J_c. If the concentration blobs did not interact and constituted an ideal gas, such deviations from the Kratky plateau would be absent. Therefore, these deviations signal the residual interaction among the concentration blobs, which generally is ignored in qualitative considerations based on the blob model. The theory thus predicts that the "plateau" in the Kratky plot $q^2S(q)$ versus q shows definite structure.

The occurrence in appropriate limits of such singular contributions is not a feature specific to polymer solutions. Viewing the excluded volume problem in the larger context of critical phenomena, one finds that the singularity found here is the analogy of a Goldstone singularity,[35] which should show up in magnetic systems close to the magnetization curve, provided we are not in the Ising universality class.[36] Due to severe experimental difficulties such singularities do not seem to have been observed up to now.

In Appendix A we give the explicit expressions for the scaling functions to one loop order in all the crossover regime, i.e., also outside the excluded volume limit. The expressions involve some complicated integrals which have to be evaluated numerically. A parametrization of the numerical results in three dimensions can be found in ref 4.

To close this theoretical section, we present the argument leading to the prediction of eq 2.11, or to $g^{\text{inter}}(r) \sim r^{3-2/\nu-\omega_{12}}$, equivalently. Such power laws are strictly valid only in the excluded volume limit where the scaling laws in eqs 4.6 and 4.7 hold. From eq 2.13 we then immediately find the scaling law

$$g^{\text{inter}}(\mathbf{r}) = g^{*\,\text{inter}}(r/R_g(0),s) \qquad (4.13)$$

We now invoke the result[16] for the number of interchain contacts in a two-chain system

$$\sigma_2 = \sum_{i,j=1}^{N} \langle \delta(\mathbf{r}_{i1} - \mathbf{r}_{j2}) \rangle \sim N^{-\nu\omega_{12}} \qquad (4.14)$$

Here it is understood that the two chains occupy the same volume of size $\sim R_g^3$. Furthermore, if we take into account the finite segment size, the δ function in eq 4.14 should be interpreted to mean that the two segments $\mathbf{r}_{i1}$ and $\mathbf{r}_{j2}$ approach each other at a distance on the order of b. Comparing eqs 2.12 and 4.14, we find that σ_2 can be expressed in terms of g^{inter} for $r \approx b$. Working in the dilute limit, we clearly have to take $s = c_p R_g^{\,3} = 0$, but due to the constraint that the chains occupy the same volume the factor of ρ in eq 2.12 has to be interpreted as the average segment density in a polymer coil: $\rho \approx N/R_g^3$. We then find

$$\sigma_2 \sim (N^2/R_g^{\,3}) g^{*\,\text{inter}}(b/R_g,0) \qquad (4.15)$$

Now assuming the power law

$$g^{*\,\text{inter}}(x,0) \sim x^{\alpha} \quad \text{for} \quad x \ll 1 \qquad (4.16)$$

and furthermore assuming that this law holds down to scales on the order of b/R_g, we find from eqs 4.14, 4.15, and 4.16

$$N^{-\nu\omega_{12}} \sim N^{2-3\nu}(b/bN^{\nu})^{\alpha} \quad \text{or} \quad \alpha = 2/\nu - 3 + \omega_{12} \qquad (4.17)$$

which is the desired result, established in the dilute limit. To argue for this result for all overlap, we note that for $r \ll \xi_d$ we test correlations among two chains deep inside a blob. The other chains are at a distance on the order of ξ_d and should not influence the local two-chain correlations, just as they do not influence the local correlations within a single chain. The overlap should show up only in the prefactors of the power law r^{α}. Indeed, in the semidilute limit even the prefactor can be determined. Here g^{inter} for $r \ll \xi_d$ should depend on chain length and overlap only via the segment density ρ. With $s = c_p R_g^{\,3} \approx \rho N^{3\nu-1}$ this yields

$$g^{*\,\text{inter}}(r/R_g,1) \sim (r/R_g)^{\alpha}(\rho N^{3\nu-1})^{\alpha\nu/(3\nu-1)} \sim \rho^{\nu\alpha/(3\nu-1)} r^{\alpha} \qquad (4.18)$$

equivalent to the simple prediction[17]

$$g^{\text{inter}}(r/R_g,s\to\infty) \sim (r/\xi)^{\alpha} \qquad r/\xi \ll 1 \qquad (4.19)$$

This result differs from the prediction (eq 2.10) of Jannink et al.[19] and in Appendix B we give a short discussion to clarify the issue.

We finally note that a law similar to eq 4.14 holds for the number of contacts σ_{co} among the two halves of the same chain[16]

$$\sigma_{co} \approx A + BN^{-\nu\omega_{12}} \qquad (4.20)$$

The constant contribution A is due to contacts of segments close to the center of the chain. Segments

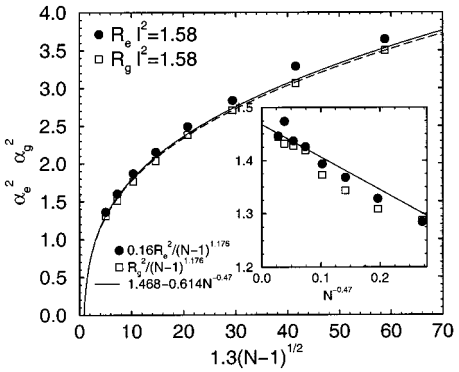

Figure 1. Swelling ratios of isolated chains ($\rho < 0.02\rho^*$). Circles denote the squared end-to-end distance $\alpha_e^2 = \langle R_e^2\rangle/[6\tilde{l}^2(N-1)]$, and squares correspond to the radius of gyration $\alpha_g^2 = \langle R_g^2\rangle/\tilde{l}^2(N-1)$. The solid line corresponds to the field theoretical result of ref 39 for α_e, and the dashed line shows the prediction of the same approach for α_g with $l^2 = 1.58$ and $\tilde{v} = 1.3$. The inset shows only first-order corrections according to $R^2 \sim (N-1)^{\nu}(1 - (\text{const})N^{-\nu\omega})$, where we have used $\langle R_g^2\rangle/\langle R_e^2\rangle = 0.16$ according to ref 7.

Table 1. Single-Chain Properties in the MC Simulations

N	$R^2_{g,MC}$	$R^2_{e,MC}$	N	$R^2_{g,MC}$	$R^2_{e,MC}$
16	194	31.1	256	6028	960
32	471	74.2	512	13756	2186
64	1117	175.6	1024	31915	4960
128	2595	409	2048	70801	11317

Table 2. Parameters of the Semidilute Systems Considered in the MC Simulations and the RG Calculations

N	ρ	s	$R^2_{g,RG}$ (s)	$R^2_{g,MC}$	$\tilde{z}$
2048	0.0032	0.287	7004	7814	58.8
2048	0.0122	1.097	5049	5715	58.8
256	0.0125	0.395	574.2	674	20.76
128	0.0125	0.278	271.6	319	14.65
64	0.0125	0.194	125.6	148	10.3

spaced far along the chain yield the correction term $BN^{-\nu\omega_{12}}$, which shows the same power law as σ_2. We have tested this prediction in our simulations, as will be discussed below.

V. Comparison between MC Results and RG Calculations

A. Isolated Chains. We now turn to the comparison among RG theory and MC data. In Figure 1 and Table 1 we present the scaling of the chain dimensions with the chain length in the range $N = 16, ..., 2048$.[38] Within the statistical accuracy on the order of 2% the data for $N \geq 256$ comply with the scaling behavior $R \sim (N-1)^{\nu}$ with $\nu = 0.588$. Also the ratio $\langle R_g^2\rangle/\langle R_e^2\rangle$ reaches the value 0.16 as expected for a self-avoiding chain.[7] For the detailed comparison we first have to determine the two nonuniversal parameters $\tilde{l}$ and $\tilde{z}$ in the RG calculations. This is carried through by analyzing the data for the radii of gyration of isolated chains. A first glance at the inset shows that $R_g^2(s{=}0)$ reaches the asymptotic power law $R_g^2 \approx N^{2\nu}$ from below. For finite chain lengths, the radius of gyration grows faster upon increasing the chain length than expected in the asymptotic excluded volume limit. This implies that the data are on the strong coupling branch of the RG flow: $u/u^* = f > 1$. The simulation data are compatible with $\langle R_g^2\rangle/(N-1)^{2\nu} \approx 0.16\langle R_e^2\rangle/(N-1)^{2\nu} \approx 1.47 - 0.61N^{-\nu\omega}$, where $\omega = 0.8$ denotes the single-chain correction to the scaling exponent. We then fit the data for $N \geq 256$ to

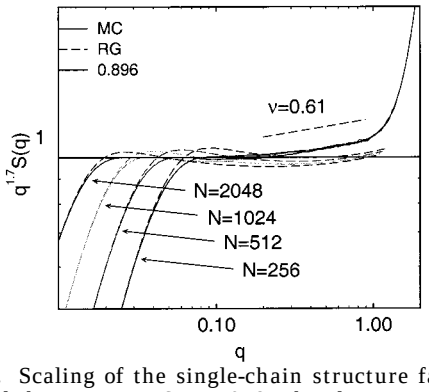

Figure 2. Scaling of the single-chain structure factor $S(\mathbf{q})$ for isolated chains $N = 256, ..., 2048$. The plateau corresponds to the Flory exponent $\nu = 0.588$. Solid lines denote the MC data, while dashed lines correspond to the RG calculations.

the theoretical swelling factor[39] (cf. the main panel of Figure 1)

$$\alpha_e^2 \equiv \frac{\langle R_e^2\rangle}{6\tilde{l}^2(N-1)} = 0.851\tilde{z}^{2(2\nu-1)}(1 - 0.53\tilde{z}^{-2\nu\omega} - 0.2247\tilde{z}^{-1-2\nu\omega}) \quad \text{with} \quad \tilde{z} = \tilde{v}\sqrt{N}$$

$$\alpha_g^2 \equiv \frac{\langle R_g^2\rangle}{\tilde{l}^2(N-1)} = 0.843\tilde{z}^{2(2\nu-1)}(1 - 0.54\tilde{z}^{-2\nu\omega} - 0.2376\tilde{z}^{-1-2\nu\omega}) \quad (5.1)$$

which yields $\tilde{v} = 1.3$ and $\tilde{l}^2 = 1.58$. As is typical for such fits, the combination $\tilde{l}^2\tilde{v}^{4\nu-2}$, which is the only parameter occurring in the excluded volume limit $u = u^*$, is determined with high precision: $\tilde{l}^2\tilde{v}^{4\nu-2} = 1.73(4)$. $\tilde{v}$ (or equivalently $\tilde{l}$) is determined by the deviations from the asymptotic limit and can be estimated only with much lower accuracy. Changes on the order of 10−20% in $\tilde{v}$ give equally good fits. Once $\tilde{v}$ and $\tilde{l}$ are given, the RG theory predicts definite results for all observables.

We should note that a one-loop calculations as underlying eqs 5.1 is known to overestimate the ratio R_g^2/R_e^2 by about 3%. Thus, not both α_e^2 and α_g^2 can consistently be fitted with the same precision. Being interested in the density correlations, we chose to extract the parameters from a fit of α_g^2.

To investigate the structure on different length scales in more detail, we present the scaling of the single-chain structure factor in Figure 2. The solid lines correspond to the MC data, while the dashed lines present the results of the RG calculations. The plateau in the $q^{1/\nu}S(\mathbf{q})$ versus q indicates that intramolecular correlations for momenta smaller than 0.2 are well describable by the exponent $\nu = 0.588$. In the range $0.2 < q < 0.9$ the correlations are compatible with a slightly larger effective exponent ($\nu \approx 0.61$). The RG results are in reasonable agreement with the MC data except for large momenta, where the microscopic properties of the bond fluctuation model dominate.

As mentioned above according to RG theory, the number of contacts among the two halves of an isolated chain in the excluded volume limit behaves like $\sigma_{co} = A + BN^{-\nu\omega_{12}}$, where the exponent $\omega_{12} \approx 0.40$ has been calculated by third-order ϵ expansion, improved by Borel resummation.[14] In the MC simulations we define that two monomers are in contact if their distance is smaller than $\sqrt{6}$. Figure 3 displays the results of the simulation. The data are compatible with a behavior of the form of eq 4.20 with $\omega_{12} = 0.4$. Fitting a power law to the

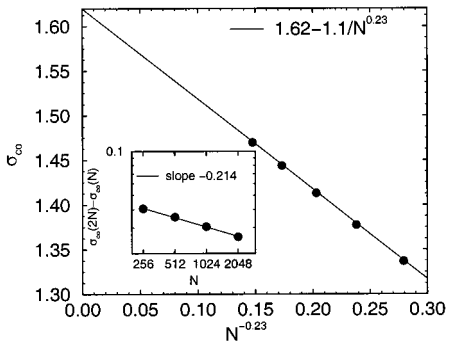

Figure 3. Scaling of the number of contacts between the different halves of a single chain. The MC data are compatible with the correction to scaling exponent $\omega_{12} = 0.4$. The inset shows a fit to the difference $\sigma_{co}(2N) - \sigma_{co}(N)$ versus N and yields $\omega_{12} = 0.36$.

difference of the number of contacts $\sigma_{co}(2N) - \sigma_{co}(N)$, we find a slightly smaller exponent, $\omega_{12} = 0.36$. We are not aware of any previous work trying to estimate this exponent from MC simulations. The deviations between the MC result and the RG calculations are not unexpected; rather large corrections to the scaling behavior for these small chain lengths have to be anticipated. Moreover, the value of σ_{co} for $N = 4096$ is likely to be too large, because of the finite system size. Finally we should note that also the theoretical estimate of ω_{12} could be changed by small higher order corrections.

B. Single-Chain Properties in Semidilute Solutions. The single-chain structure factor in semidilute solutions is presented in the Kratky form in Figure 4a. The radius of gyration is 88.4 and 75.6 for $L = 400$ and 256, respectively. Hence, the ratio between the density and its crossover value to the dilute regime $\rho/\rho^* \equiv 3N\rho/4\pi R_g^3$ is 4.5 for $L = 400$ and 11 for $L = 256$. A plateau in $q^2S(\mathbf{q})$ indicates the screening of the excluded volume interaction and Gaussian intramolecular correlations. The plateau values expected from the Debye approximation are $2N/R_g^2 = 0.52$ and 0.72, respectively.

Such a plateau is clearly detectable for the smaller system size (or higher density) in the range $0.04 < q < 0.31$; however, there is some additional structure in the plateau (which we shall discuss in detail below). The dashed line $q^2S(q) \sim q^{2-1/\nu}$ represents the statistics of a self-avoiding chain. From the intersection of that line with the Kratky plateau (for which we use the effective value 0.64), we extract the screening length $\xi(L{=}256) = 20.3$. For $q > q_b = 0.9$ deviations from the self-avoiding scaling behavior become important; this marks the microscopic length scale. It corresponds to a distance $b = 7$ which exceeds the bond length of our model by a factor of 2.7. For $L = 256$ the screening length exceeds the microscopic length scale by about a factor of 2.9. Increasing the density further, we would decrease the screening length and enter the regime of concentrated solutions.

For the larger system size the plateau in the Kratky plot is not well developed. If we estimate the plateau value to 0.48, we obtain $\xi(L{=}400) = 53$ for the screening length. Since the radius of gyration R_g exceeds the screening length ξ only by a factor of 1.7, no pronounced plateau in $q^2S(q)$ can be expected. For larger momenta ($q > 0.2$) the data are described by the same self-avoiding chain asymptote as the chains in the smaller system. Of course, this is expected, because on length scales smaller than the screening length, intramolecular excluded volume interactions dominate. Decreasing the density further, we would increase the screening length and enter into the dilute regime. Hence, the two systems studied mark the regime of semidilute solutions for chain length $N = 2048$. The RG results are also shown in the figure. In qualitative agreement with the MC simulations we observe some structure in the region of the Kratky plateau, and $2N/R_g^2$ overestimates the plateau value.

To investigate the intramolecular correlations in more detail, we plot the ratio $ND(q^2R_g^2)/S(q)$ in Figure 4b,c, where

$$D(x) = (2/x^2)[\exp(-x) - 1 + x] \qquad (5.2)$$

is the Debye function. In these plots we consistently used $R_g(s)$ as calculated from the RG theory for the given overlap of the systems. Panel b corresponds to chains of length $N = 2048$, and we vary the density, and part c shows the corresponding plots for systems of density $\rho = 0.0125$ and chain lengths $N = 64$, 128, and 256. The relevant values of $\tilde{z}$ and of $R_g^2(s)$ and $(4\pi/3)\pi s = c_p(4/3)\pi R_g^3(s{=}0)$ are given in Table 1.

Both plots concentrate on the deviations from the Debye approximation, which are due to two sources: Our crossover condition for l_R incorporates the correct large-momentum behavior of the single-chain structure factor S. Specifically in the excluded volume limit $S(q) \sim q^{-1/\nu}$, $q \to \infty$, so that $ND(q^2R_g^2)/S(\mathbf{q})$ decreases like $q^{1/\nu-2} \approx q^{-0.299}$. This effect is incorporated already in the zero-loop approximation of our theory. In the small-momentum region the deviations from the Debye function, however, are due to the one-loop corrections. The most important feature of these figures is the pronounced hump visible in ND/S due to the Goldstone singularity. This magnifies the structure seen in the plateau in the Kratky plot. The structure revealed by the MC simulations is even more pronounced than predicted by the one-loop theory, but qualitatively the shape of the simulational and the theoretical curves is most similar. The agreement between RG theory and MC data is not quantitative, however, and we will comment on possible sources of the discrepancy in the discussion.

Another comparison between the Gaussian structure on large length scales and the self-avoiding chain statistics is presented in Figure 4d for chain length $N = 2048$. In the limit $q \to 0$ the Debye function[40] and the structure factor agree if we use a Gaussian chain of equivalent number of monomers and radius of gyration. For $q\xi > 1$ the Debye function decays such as q^{-2}, while the single-chain structure factor decreases like $q^{-1/\nu}$. Therefore, the Debye function underestimates $S(q)$ for large wave vectors. Since $\int d^3q\, S(q)$ is normalized, the Debye function has to overestimate $S(q)$ for smaller wave vectors $q\xi < 1$ in qualitative agreement with the data in Figure 4d.

C. Intermolecular Correlations: Structure Factor and Pair Correlation Function. We next consider the interchain correlations. The single-chain properties show that the momentum regime $2\pi/\xi < q < 0.9$ characterizes the length scale between the microscopic structure and the screening length. The lower bound depends on ρ and takes the value 0.1 for $L = 400$ and 0.3 for $L = 256$ and $N = 2048$. Inside this "blob" [9] the probability of finding a monomer of the same chain is much higher than that of finding a monomer of a different chain. This intermolecular packing inside the blob is investigated in this section.

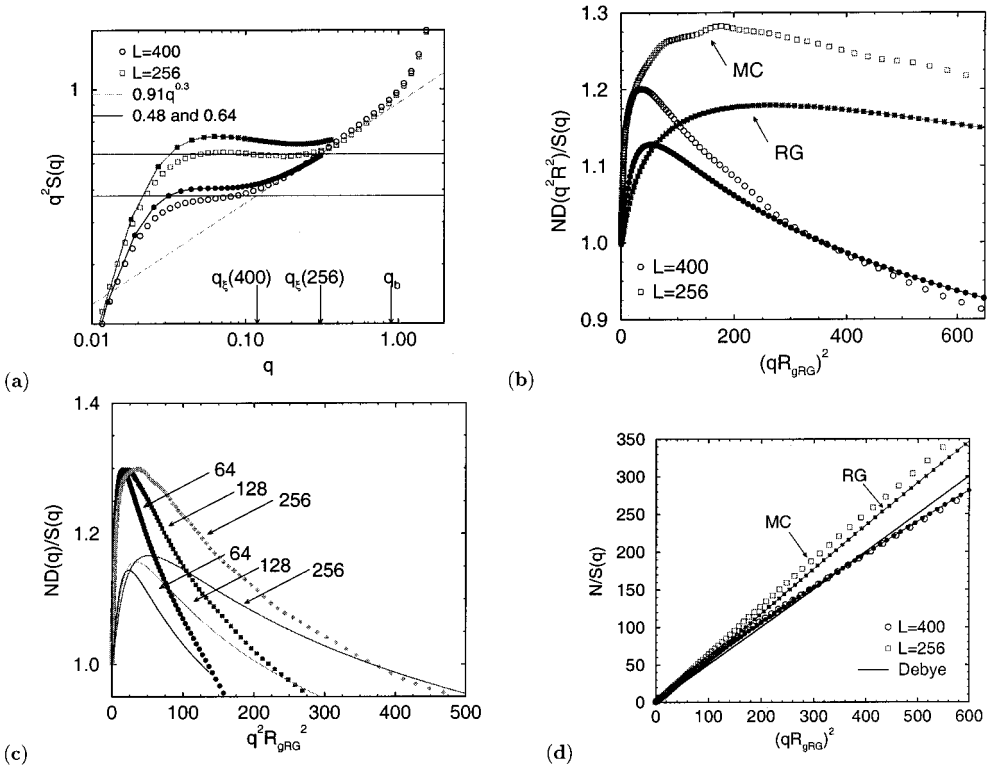

Figure 4. Single-chain structure factor in a semidilute solution. (a) Kratky plot for chain length $N = 2048$ and linear extension of the simulation box $L = 400$ and $L = 256$. The arrows on the q axis mark the microscopic length scale $b = 7$, and the screening lengths $\xi = 53$ and 20.3 for the monomer number densities $\rho = 0.0122$ and 0.0032, respectively. Open symbols refer to the MC data; lines with filled symbols denote the results of the RG calculations. (b) Ratio of the Debye function using the RG prediction for the chain extension and the single-chain structure factor in the MC simulations and RG calculations at fixed chain length $N = 2048$ and $\rho = 0.0122$ and 0.0032. Symbols as in (a). (c) Ratio of the Debye function using the RG prediction for the chain extension and the single-chain structure factor in the MC simulations and RG calculations at fixed monomer density $\rho = 0.0125$ and chain lengths $N = 64$, 128, and 256. Symbols denote the MC results, while lines correspond to the RG calculations. (d) Inverse structure factor for $N = 2048$ and $\rho = 0.0122$ and 0.0032. Symbols as in (a).

The structure factors of the system sizes $L = 400$ and $L = 256$ and chain length $N = 2048$ are presented in Figure 5a,b, respectively. In this Kratky form the plateau in $S(\mathbf{q})$ at small q values marks the Gaussian correlations on length scales larger than the screening length. The coherent structure factor $G(\mathbf{q})$ approaches the single-chain structure factor with increasing $\mathbf{q}$, and the difference—the distinct part $H(\mathbf{q})$—decreases rapidly. The decrease appears to be faster than the prediction of Jannink et al.,[19] $H(\mathbf{q}) \sim q^{-3}$, but slower than the RPA prediction for Gaussian chains, $H(\mathbf{q}) \sim q^{-4}$. The RPA-like scaling of the distinct part $H(\mathbf{q})$ is presented in part c. For $q\xi > 10$ the data are compatible with $H(\mathbf{q}) \sim q^{-3-\alpha}$ with $\alpha = 0.4, \ldots, 1$. Using the RPA-like form of the structure factor, we can estimate an effective interaction parameter v. As suggested by scaling arguments and P-RISM calculations the effective interaction depends on the density. In panel d, we plot

$$\left(\frac{1}{G(\mathbf{q})} - \frac{1}{S(\mathbf{q})}\right)\rho^{-1/(3\nu-1)} \tag{5.3}$$

versus $q\xi$ and we obtain a fair data collapse for the two densities. According to the unrenormalized RPA this difference would be a constant, proportional to the segment density to the power $1 - 1/(3\nu - 1) = -0.31$. Renormalization of the RPA changes the density dependence $v\rho \rightarrow u^*\rho^{1/(3\nu-1)}$ in the excluded volume limit, and this motivates the scaling in the figure. Renormalization also introduces some weak momentum dependence of the effective coupling: on the strong coupling branch $f = u/u^* > 1$ increases weakly with decreasing l_R, i.e., increasing q. The result of renormalized RPA is shown by the broken lines in Figure 5d. The one-loop correction inverts this trend and leads to a stronger decrease, in full accord with the MC data. This momentum dependence of v indicates the failure of the renormalized RPA[18,20,21] and P-RISM[17] theories to capture correctly the intermolecular correlations. A decrease of the effective interaction parameter with q was also found in the simulations of Yamakov et al.;[22] however, the data also showed a q dependence for small q vectors. This is not found in the momentum range which we have investigated and might be caused by insufficient relaxation of long-range density fluctuations in ref 22.

The real-space analogy of the distinct part of the intermolecular scattering function is shown in Figure 6a for the two densities and chain length $N = 2048$. In the RG calculations we obtain the intermolecular correlations in r space via a numerical Fourier transform of $H(\mathbf{q}) = G(\mathbf{q}) - S(\mathbf{q})$. To roughly take into account the lattice used in the MC simulations, we cut off the q integration at $q^2 = 3\pi\beta^2$, where $\beta = 6/\pi$ is determined by comparing the radius of a sphere to the length of the edge of a cube of the same volume. At the cutoff, $H(\mathbf{q})/N$ is very small: $H(\mathbf{q})/N \approx 10^{-4}$. Again we find good quantitative agreement in the entire range of distances r.

One notes immediately that the contact value of the intermolecular pair correlation function $g^{\text{inter}}(\mathbf{r})$ is very small. On the scale $b < r < \xi$ the distinct part of the scattering function decays like $(q\xi)^{-3-\alpha}$, and this corre-

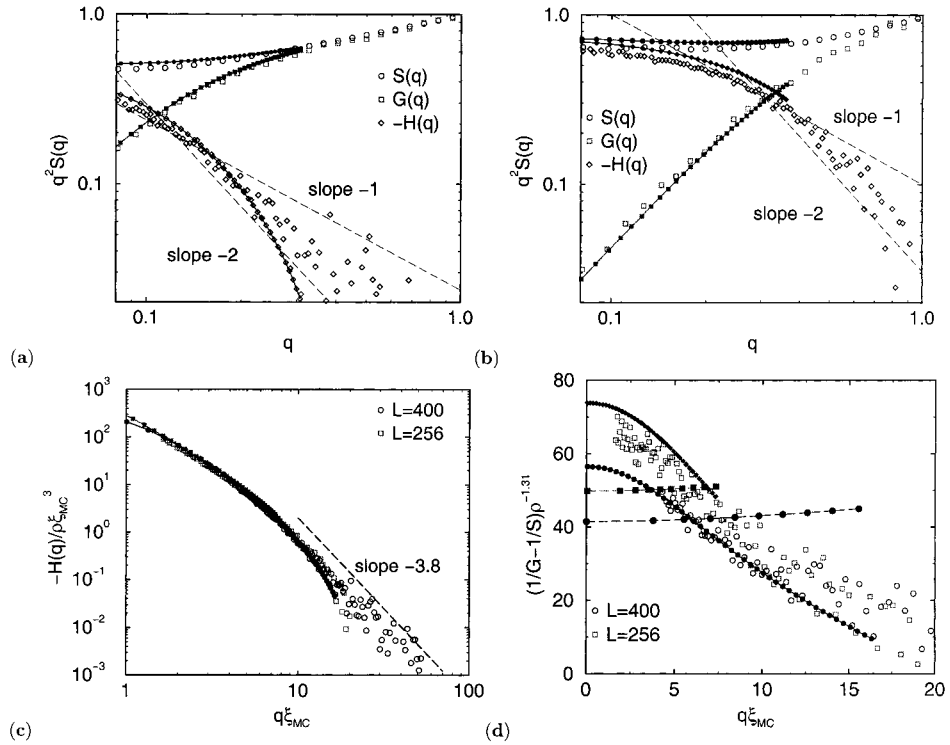

Figure 5. Intra- and intermolecular structure factors for chain length $N = 2048$ and (a) $L = 400$ and (b) $L = 256$. Circles denote the single-chain structure factor $S(\mathbf{q})$, squares refer to the coherent structure factor $G(\mathbf{q})$, and diamonds represent the distinct part $H(\mathbf{q})$. Open symbols show the MC results, while lines with filled symbols display the results of the RG calculations. The straight lines without symbols with slopes −1 and −2 correspond to $H \sim q^{-3}$ and $H \sim q^{-4}$, respectively. (c) Scaling of the distinct part of the structure factor. Circles refer to $L = 400$, and squares show the results for $L = 256$. Open symbols represent the MC simulations, while filled symbols display the RG results. For $q\xi > 8$ the data are well describable by a decay with a power of 3.8. (d) Scaling and momentum dependence of the effective interaction parameter v. Symbols as in (c). The lines with positive slope correspond to the renormalized RPA results.

sponds to $g^{\text{inter}}(\mathbf{r}) \sim (r/\xi)^{\alpha}$. On large length scales ($r > \xi$) the pair correlation function g^{inter} is dominated by the radius of gyration. On this length scale the behavior is similar to that in a melt. The total density is constant; the density distribution of the monomers along a chain is exactly balanced by the correlation hole in the intermolecular pair correlation function.[10,17] This suggests that the large length scale behavior of the intermolecular pair correlation function is given by

$$g^{\text{inter}}(\mathbf{r}) = 1 - \frac{\xi}{r} f\left(\frac{r}{R_g}\right) \quad \text{for} \quad r \gg \xi \tag{5.4}$$

For $r \approx \xi$ there is a smooth crossover to the power-law behavior on smaller distances. The $1/r$ dependence matches the $1/q^2$ decay of the single-chain structure factor on the scale $\xi < r < R_g$. Moreover, the decay on large length scales $\int d\mathbf{r}^3\, \rho(g^{\text{inter}} - 1) \sim \rho\xi R_g^2 \sim N$ ensures that the correlation hole contains N monomers. These two scaling behaviors are tested in Figure 6b on the large length scale and Figure 6c on short distances. In view of the rather large uncertainty in the screening length for the larger system ($L = 400$) and corrections to scaling due to the finite ratios b/ξ and ξ/R_g the data collapse is good. The correlation hole at small distances r is not quite as strong in the MC simulations as predicted by the RG theory. This partly may be due to lattice effects. In the plots the lattice constant is on the order of $1/R_g \approx 0.015$ or $1/\xi \approx 0.03$, respectively.

The small distance data also represent a sensitive test of the expected power-law behavior. A doubly logarithmic plot of g^{inter} is presented in Figure 6d. Due to a finite microscopic length scale we anticipate a shift in the abscissa by two lattice constants. This corresponds to the monomer extension and results in a rather extended power-law behavior on small distance. A power law fit to the small r scaling yields the exponent $\alpha \approx 0.73$. Due to the shift of the origin and the finite ratio b/ξ, the uncertainty in the exponent α is rather large and the data are compatible with the exponent $0.4 < \alpha < 1$. However, a logarithmic increase ($\alpha = 0$) of $g^{\text{inter}}(\mathbf{r})$ as predicted by Jannink et al.[19] appears to be incompatible with our simulation data. The renormalized RPA/P-RISM yields the exponent $\alpha = 2/\nu - 3$, which gives 0.4 for $\nu = 0.588$ and 1 for Gaussian chains. Numerically, both values are compatible with our simulation data within the rather large error for the exponent α. However, the MC data lend stronger support to the value $\alpha = 2/\nu - \omega_{12} - 3 = 0.80$. This observation is also compatible with the decay of the distinct part of the structure factor observed in the previous simulations by Yamakov et al.[22]

VI. Discussion and Outlook

We have investigated intra- and interchain correlations in semidilute polymer solutions via MC simulations of rather long chains, $N = 2048$, in the bond fluctuation model and RG calculations. The two parameters $\tilde{z}$ and $\tilde{l}$ of the RG calculations were identified via the chain length dependence of the chain extension in the dilute regime. This allows for a comparison between the RG calculations and the MC simulations for the correlation functions without adjustable parameters. On the length scale between the screening length ξ and the microscopic length b the scaling of the intermolecular correlations is dominated by the screening length ξ, and

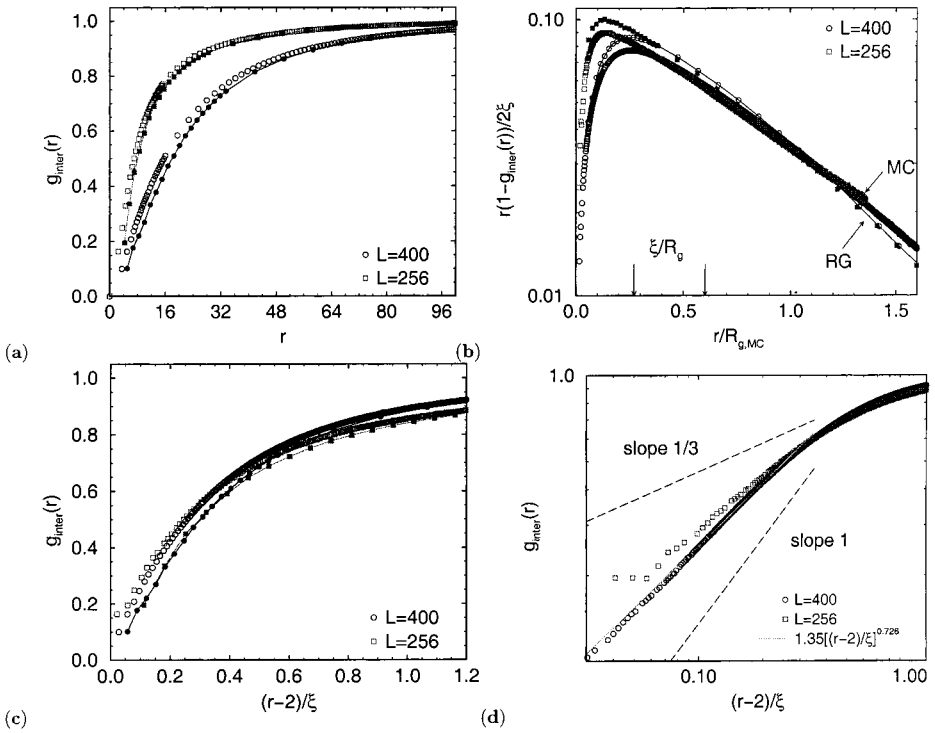

Figure 6. Real space dependence of the intermolecular correlations: (a) Intermolecular pair correlation function $g^{\text{inter}}(r)$ for chain length $N = 2048$ and $\rho = 0.0032$ ($L = 400$) and $\rho = 0.0122$ ($L = 256$). Open symbols correspond to the MC results, whereas filled ones represent the RG calculations. (b) Scaling of $g^{\text{inter}}(\mathbf{r})$ at large distances $r > \xi$. The values of the screening length in units of the radius of gyration are indicated by arrows on the r axis. Symbols as in (a). (c) Scaling of $g^{\text{inter}}(\mathbf{r})$ at small distances $r < \xi$. $g^{\text{inter}}(\mathbf{r})$ does not attain a finite, constant value in the range $b < r < \xi$. Symbols as in (a). (d) Power-law dependence of $g^{\text{inter}}(\mathbf{r})$ at small distance. The data are compatible with a dependence of the form $g^{\text{inter}}(\mathbf{r})$ with exponent $\alpha = 0.7(3)$. Symbols as in (a).

the intramolecular correlations are that of a self-avoiding walk. Both MC simulations and RG calculations show deviations from the plateau in the Kratky plot $q^2S(q)$ versus q. To our knowledge this is the first observation in the realm of critical phenomena of a structure which must be traced back to a Goldstone-type singularity.[36] These deviations from the plateau in the Kratky plot indicate deviations from the Gaussian behavior on intermediate length scales. In semidilute solutions of linear chains they are due to small (not dominant, in a scaling sense) interactions between excluded volume blobs on length scales larger than the screening length.[41]

The distinct part of the coherent scattering function decreases like $(q\xi)^{-3-\alpha}$ for $q\xi > 1$ and the intermolecular correlation function increases like $(r/\xi)^{\alpha}$ with $0.4 < \alpha < 1$. The value $\alpha = 0$, as proposed by Jannink and co-workers,[19] appears to be inconsistent with our simulations. The numerical value of α in the simulations is compatible with the renormalized RPA[18,20,21] or P-RISM[17] prediction $\alpha = 2/\nu - 3 = 0.4$, though the data are in better agreement with the value $\alpha = 2/\nu + \omega_{12} - 3 = 0.8$, where $\omega_{12} \approx 0.4$ denotes the two molecule corrections to scaling exponent. This law results from the current implementation of the short distance expansion within the renormalized theory. On distances larger than the screening length ξ the intramolecular correlations are approximatively Gaussian and the intermolecular pair correlation function depends on two length scales—the radius of gyration and screening length. A simple scaling form (eq 5.4) has been compared to the MC simulations. Further simulations and experiments on ternary mixtures of two polymers in a common solvent might contribute to understanding the intermolecular packing.

To close, we again turn to the intramolecular correlations and consider possible sources of the discrepancies among the RG theory and the simulation data. First, we want to stress that this discrepancy in fact is not very strong. The plots magnify the one-loop corrections. Some deviations may arise from the uncertainty in the parameters $\tilde{l}$ and $\tilde{z}$ required for mapping between the MC model and the RG calculations. Moreover, since the structure considered first occurs in one-loop order, it is well conceivable that a higher order calculation will change the theoretical result somewhat. We clearly expect to find higher loop corrections to the amplitude of the Goldstone singularity. However, there are also corrections connected to the finite size of the simulation volume. The ratio of the end-to-end distance of the chains to the size of the box is on the order of $R_e/L \approx 2$, and therefore standard finite size corrections could play some role. More important is the fact that the simulation treats a canonical ensemble of 100 chains of length 2048, whereas the theory evaluates a grand canonical ensemble in the thermodynamic limit. In a finite size system more directly related to the theory the number of chains therefore should fluctuate by about ± 10. Suppressing these fluctuations in a finite ensemble certainly will have consequences for the scaling function, which go beyond standard finite size effects. In this context it is of interest to observe that the measured radii of gyration at finite concentration definitely are larger than the theoretical predictions (cf. Table 1). The deviations are larger than expected from our experience with the performance of the renormalized one-loop approximation. Indeed, as shown in Figure 18.5 of ref 4, the few data on $R_g^2(s)$ available from physical experiments are quite consistent with the theoretical scaling function. The deviations found in the present simula-

tions may indicate that the efficiency of screening is reduced in the finite canonical ensemble, and support the view that finite size effects cannot be ignored.

Acknowledgment. It is a great pleasure to thank M. Fuchs, J. Baschnagel, A. Milchev, and J. P. Wittmer for stimulating discussions and helpful correspondence. Financial support by the Deutsche Forschungsgemeinschaft Bi314-17 and SFB 237 and generous access to the CRAY T3E at the HLR Stuttgart and HLRZ Jülich and the CONVEX SPP2000 at the Rechenzentrum Mainz are gratefully acknowledged.

Appendix A: Explicit One-Loop Results

We here collect previously established results for the renormalization group mapping and the scaling functions. These results extensively are discussed in a recent publication,[4] where it also has been shown that the theory in the form presented here is well confirmed by experiment.

1. Renormalization Group Mapping. As physical scaling variables we use

$$\tilde{z} = \tilde{\nu} N^{1/2}, \quad \tilde{s} = c_p \tilde{R}_0^{\,3}, \quad q^2 \tilde{R}_0^{\,2}$$

where $\tilde{R}_0 = \tilde{l} N^{1/2}$. The renormalization group maps these variables onto renormalized counterparts f, N_R, and $\bar{q}^2$, according to the equations (see ref 4, section 13.3)

$$\tilde{z} = f|1-f|^{-1/2\nu\omega} H_u(f)\, H^{-1/2}(f)\, N_R^{\,1/2} \tag{A1}$$

$$q^2 \tilde{R}_0^{\,2} = |1-f|^{(2-(1/\nu))(1/\omega)} H^{-1}(f)\, N_R \bar{q}^2 \tag{A2}$$

$$\tilde{u}\tilde{s}\tilde{z} = |1-f|^{(1/\omega)(3-(2/\nu))} H_u(f) \times H^{-2}(f)\, c_0 N_R \left(1 - \frac{\bar{q}^2}{q_0^{\,2}} - \frac{n_0}{N_R}\right) \tag{A3}$$

where the exponents take the values

$$\frac{1}{\omega}\left(3 - \frac{2}{\nu}\right) = -0.502; \quad \frac{1}{2\nu\omega} = 1.063; \quad \left(2 - \frac{1}{\nu}\right)\frac{1}{\omega} = 0.374$$

The constant $\tilde{u}$ is defined as

$$\tilde{u} = (4\pi)^{3/2}(u^*/2) = 8.107$$

and c_0, n_0, and q_0^2 are theoretical parameters which fix the crossover from dilute to semidilute systems (c_0), from Θ systems to excluded volume systems (n_0), and from small to large momenta (q_0^2). In previous work we adjusted these parameters to find good results for certain universal ratios, which leads to the choice

$$n_0 = 0.53; \quad c_0 = 1.2; \quad q_0^{\,2} = 50$$

Finally the functions

$$H_u(f) = (1 + 0.824 f)^{0.25}$$

$$H(f) = 1 - 0.005 f - 0.028 f^2 + 0.022 f^3$$

are numerical parametrizations of a Borel-resummed form of a high-order calculation of the renormalization group flow.

The coupling parameter f reaches the value $f = 1$ in the excluded volume limit. The weak coupling branch $0 < f < 1$ interpolates among Θ conditions and excluded volume conditions, and $f > 1$ is the strong coupling branch. N_R is the renormalized chain length, taking values $N_R = 1$ or $N_R = \infty$ in the dilute ($\tilde{s} = 0$) or semidilute ($\tilde{s} = \infty$) limits. Finally $\bar{q}^2$ governs the crossover in momentum from the small momentum limit ($q^2\tilde{R}_0^2 = 0$; $\bar{q}^2 = 0$) to the limit of large momenta ($q^2 = \tilde{R}_0^2 \to \infty$, $\bar{q}^2 \to q_0^2$). To evaluate the mapping, we solve eqs A1 and A2 for N_R or $\bar{q}^2$, respectively, and we substitute the results into eq A3 to find an implicit equation for $f = f(\tilde{z},\tilde{s},q^2\tilde{R}_0^2)$. The physical scaling functions take the form of power series in f, with coefficients depending on N_R and $\bar{q}^2$.

2. Scaling Functions. The scaling functions have been evaluated in the loop expansion to one-loop approximation. We first quote the results for the scaling function of the density autocorrelations (ref 4, chapter 18)

$$J_a(q^2\tilde{R}_0^{\,2},\tilde{s},\tilde{z}) = (1/N)S(q)$$

We write J_a in the form

$$J_a = D(\hat{Q}) \tag{A4}$$

where

$$D(x) = (2/x^2)(e^{-x} - 1 + x) \tag{A5}$$

is the Debye function. The variable $\hat{Q}$ is given as

$$\hat{Q} = \bar{\mathbf{q}}^2 N_R [1 - u^* f (1 + (1/2) N_R^{\,1/2} M_a(\bar{\mathbf{q}}^2 N_R, W_R))] \tag{A6}$$

where

$$W_R = c_0 (N_R - n_0 - (\bar{q}^2/q_0^{\,2}) N_R) \tag{A7}$$

The function M_a is determined by numerical evaluation of some complicated integral.

$$M_a(Q,W) = \left[\frac{\sqrt{\pi}}{2} Q D'(Q)\right]^{-1} \int_0^\infty dy \times y^{-1/2} \left[\frac{D(Q) - D(y)}{Q - y}\left(1 + \frac{2}{\rho(y)}\right) - W D'(Q)\frac{D(y)}{\rho(y)} + \frac{1 - e^{-y}}{y\rho(y)} D(Q) + Q H_1(y,Q)\right] + (4\pi)^{3/2}[Q D'(Q)]^{-1} \times \int \frac{d^3k}{(2\pi)^3} \frac{1}{\rho(k^2)} [H_1(K_1,k^2) + 2H_2(k^2,K_1,Q) - W D(k^2)\, H_1(K_1,Q)] \tag{A8}$$

Here

$$D'(y) = (d/dy) D(y)$$

$$\rho(y) = 1 + W D(y)$$

$$H_1(y_1,y_2) = \frac{1}{(y_1 - y_2)^2}[D(y_1) - D(y_2) - (y_2 - y_1) D'(y_2)]$$

$$H_2(y_1,y_2,y_3) = \frac{D(y_1)}{(y_2 - y_1)(y_3 - y_1)} + \frac{D(y_2)}{(y_3 - y_2)(y_1 - y_2)} + \frac{D(y_3)}{(y_1 - y_3)(y_2 - y_3)} \tag{A9}$$

With $Q = \bar{\mathbf{q}}^2 N_R$ the variable K_1 stands for

$$K_1 = (\mathbf{k} + \bar{\mathbf{q}} N_R^{1/2})^2 \quad \text{(A10)}$$

A good parametrization of the numerical results for M_a can be found in ref 4, section A 18.2.

We now turn to the scaling function for the total structure factor

$$J_c(q^2 \tilde{R}_0^2, \tilde{s}, \tilde{z}) = (1/N) G(q)$$

J_c can be written in RPA-like form

$$J_c^{-1} = J_a^{-1} + M_c(\mathbf{q}) \quad \text{(A11)}$$

J_a has been given above. For $M_c(\mathbf{q})$ we find (ref 4, section A 19.1)

$$M_c(\mathbf{q}) = W_R\{1 + u^* f[\, 2 - N_R^{1/2} M_c(\bar{q}^2 N_R, W_R)]\} \quad \text{(A12)}$$

with

$$M_c(Q,W) = \frac{1}{2}(4\pi)^{3/2} D^{-2}(Q) \times \int \frac{d^3k}{(2\pi)^3} \frac{1}{\rho(k^2)\,\rho(K_1)} \left[\frac{1}{2} H(k^2,K_1)^2 + H(k^2,Q)(2H(k^2,K_1) + H(K_1,Q) + H(k^2,Q))\right] \quad \text{(A13)}$$

The function H takes the form

$$H(y_1,y_2) = \frac{D(y_1) - D(y_2)}{y_1 - y_2} \quad \text{(A14)}$$

and the other ingredients have been defined above. A good parametrization of M_c can be found in ref 4, section A 19.2.

Appendix B: Short Distance Expansion

Basically, the argument in section IV which leads to eq 4.19 is nothing but the short distance expansion (sde), formulated directly for the polymer correlation functions. In standard form this expansion is concerned with products of operators in a field theory.[37] Using zero-component Landau−Ginzburg−Wilson field theory, the prediction in eq 2.10 has been derived in ref 19. A detailed exposition of the arguments of ref 19 is beyond the scope of our paper. Here we just give a brief discussion. The prediction in eq 2.10 is based on the sde in the form (ref 19, eq 10)

$$\phi^2\left(\mathbf{R} + \frac{\mathbf{r}}{2}\right) \phi^2\left(\mathbf{R} - \frac{\mathbf{r}}{2}\right) \approx D_1(\mathbf{r})\, \phi^2(\mathbf{R}) + D_2(\mathbf{r})(\phi^2(\mathbf{R}))^2 \quad \text{(B1)}$$

where $\phi(\mathbf{R})$ is a local fluctuating field. As is well known, the field theoretic approach is strictly equivalent to the theory of binary polymer solutions as underlying the present work. The operator $\phi^2(\mathbf{R})$, in particular, directly corresponds to the local monomer density $\rho(\mathbf{r})$. We thus apparently run into a contradiction among the direct polymer formulation and the equivalent field theoretical approach.

However, the analysis based on eq B1 misses some subtle point. It is concerned with the correlations of the *total* segment density, which, thus, in the semidilute excluded volume limit behave as (ref 19, eq 12)

$$\frac{1}{N} G(\mathbf{q}) \approx s^{-1/(3\nu-1)}[(q^2\xi^2)^{-1/2\nu} + (\text{const})(q^2\xi^2)^{-d/2} + (\text{const})(q^2\xi^2)^{-2/\nu-\omega}] \quad \text{(B2)}$$

The segments contributing to $H(\mathbf{q})$ are on *different* chains, however, and a proper formulation needs the extension of the theory to two different polymer species (i.e., a ternary solution), so as to identify the two chains. In field theory we need to introduce two different fields, $\phi_1(\mathbf{r})$ and $\phi_2(\mathbf{r})$, representing the two species, and the sde for $H(\mathbf{q})$ has to respect the fact that this observable involves both fields. Equation B1 is to be replaced by

$$\phi_1^2\left(\mathbf{r} + \frac{\mathbf{r}}{2}\right) \phi_2^2\left(\mathbf{r} - \frac{\mathbf{r}}{2}\right) \approx D(\mathbf{r})\, \phi_1^2(\mathbf{R})\, \phi_2^2(\mathbf{R}) \quad \text{(B3)}$$

The operator $\phi_1^2(\mathbf{R})\, \phi_2^2(\mathbf{R})$ is of anomalous dimension ω_{12}, and under renormalization it does not couple to other operators of the zero-component polymer field theory. Starting from eq B3 also the field theoretic formulation of the sde yields the prediction in eq 4.19 with $\alpha = 2/\nu - d - \omega_{12}$. No terms of the type ln r or $r^{2/\nu-d+\omega}$ show up. Using the explicit results for the scaling function $H(\mathbf{q})$ as given in ref 4 for all $d \le 4$, we have checked that the prediction in eq 4.19 is consistent with the expansion in $\epsilon = 4 - d$, evaluated to one-loop order.

References and Notes

(1) des Cloizeaux, J.; Jannink G. *Polymers in Solution: Their Modeling and Structure*; Oxford Science Publications: Oxford, 1990.
(2) Freed, K. F. *Renormalization Group Theory of Macromolecules*; Wiley: New York, 1987.
(3) Le Guillou, J. C.; Zinn-Justin, J. *J. Phys. (Paris)* **1989**, *50*, 1365.
(4) Schäfer, L. *Excluded Volume Effects in Polymer Solutions*; Springer: Berlin, 1999.
(5) Rajasekaran, J. J.; Muthukumar, M. *Macromolecules* **1994**, *27*, 6418.
(6) Alessandrini, J. L.; Carignano, M. A. *Macromolecules* **1992**, *25*, 1157.
(7) Li, B.; Madras, N.; Sokal, A. D. *J. Stat. Phys.* **1995**, *80*, 661. Sokal, A. D. In *Monte Carlo and Molecular Dynamics Simulation in Polymer Science*; Binder, K., Ed.; Oxford University Press: New York, 1995; Chapter 2.
(8) Onuki, A.; Hashimoto, T. *Macromolecules* **1989**, *22*, 879.
(9) de Gennes, P. G. *Scaling Concepts in Polymer Physics*; Cornell University Press: Ithaca, NY, 1979.
(10) Schweizer, K. S.; Curro, J. G. *Adv. Chem. Phys.* **1997**, *98*, 1.
(11) de Gennes, P. G. *J. Polym. Sci., Polym. Phys.* **1978**, *16*, 1881.
(12) Joanny, J.-F.; Leibler, L.; Ball, R. *Macromolecules* **1984**, *17*, 4640. Broseta, D.; Leibler, L.; Joanny, J.-F. *Macromolecules* **1987**, *20*, 1935.
(13) Schäfer, L.; Kappeler, C. *J. Phys.* **1985**, *46*, 1853. Schäfer, L.; Kappeler, C. *J. Chem. Phys.* **1993**, *99*, 6135.
(14) Schäfer, L.; Lehr, U.; Kappeler, C. *J. Phys. I* **1991**, *1*, 221.
(15) The Flory-Huggins parameter in a ternary solution comprises not only enthalpic contributions (proportional to the number of intermolecular contacts per monomer), but also contributions from the conformational entropy. However, both contributions scale in the same way.
(16) Müller, S.; Schäfer, L. *Euro. Phys. J. B* **1998**, *2*, 351.
(17) Fuchs, M.; Müller, M. *Phys. Rev.* **1999**, *E60*, 1921.
(18) Ullman, R.; Benoit, H.; King, J. S. *Macromolecules* **1986**, *19*, 183.
(19) Jannink, G.; Pfeuty, P.; Lapp, A.; Cotton, J. P. *Europhys. Lett.* **1994**, *27*, 47.
(20) Daoud, M.; Cotton, J. P.; Farnoux, B.; Jannink, G.; Sarma, G.; Benoit, H.; Duplessix, R.; Picot, C.; deGennes, P. G. *Macromolecules* **1975**, *8*, 805.
(21) Benoit, H.; Benmouna, M. *Polymer* **1984**, *25*, 1059.
(22) Yamakov, V.; Milchev, A.; Binder, K. *J. Phys. II* **1997**, *7*, 1123.
(23) Carmesin, I.; Kremer, K. *Macromolecules* **1988**, *21*, 2819. Deutsch, H.-P.; Binder, K. *J. Chem. Phys.* **1991**, *94*, 2294.
(24) Flory, P. J.; Bueche, A. M. *J. Polym. Sci.* **1958**, *27*, 219.

(25) Sariban, A.; Binder, K. *Colloid Polym. Sci.* **1994**, *272*, 1474.
(26) Paul, W.; Binder, K.; Kermer, K.; Herrmann, D. W. *J. Phys. II* **1991**, *1*, 37.
(27) Müller, M.; Paul, W. *J. Chem. Phys.* **1994**, *100*, 719.
(28) Müller, M.; Binder, K. *Macromolecules* **1995**, *28*, 1825.
(29) Kron, A. K. *Polym. Sci. USSR* **1965**, *7*, 1361. Wall, F. T.; Mandel, F. *J. Chem. Phys.* **1975**, *63*, 4592.
(30) Sokal, A. D.; Madras, N. *J. Stat. Phys.* **1988**, *50*, 109.
(31) Frenkel, D.; Smit, B. *Mol. Phys.* **1992**, *75*, 983. dePablo, J. J.; Laso, M.; Suter, U. W. *J. Chem. Phys.* **1992**, *96*, 6157.
(32) Consta, S.; Wilding, N. B.; Frenkel, D.; Alexandrowicz, Z. *J. Chem. Phys.* **1999**, *110*, 3220.
(33) Yamakawa. *Modern Theory of Polymer Solutions*; Harper and Row: New York, 1971.
(34) ξ_d and ξ show the same scaling behavior, but their numerical values differ by a factor on the order of unity. ξ is defined *via* the crossover from $S(q) \sim 1/q^2$ to $S(q) \sim 1/q^{1/\nu}$ at $q = 2\pi/\xi$. ξ_d is defined in eq 23.
(35) Goldstone modes arise in phase transitions where a spontaneous breaking of a continuous symmetry occurs (e.g., magnetic systems provided they are not in the Ising universality class) and there exists an analogy[1−4] between magnetic systems and polymer solutions. The perturbative contributions which give rise to a singular derivative in the small q expansion of J_a^{-1} directly correspond to those terms which give rise to Goldstone singularities in magnetic systems.
(36) Schäfer, L.; Müller, M.; Binder, K. Preprint.
(37) Zinn-Justin, J. *Quantum Field Theory and Critical Phenomena*; Clarendon Press: Oxford, 1989.
(38) The bond length in the bond fluctuation model is about a factor 2.6 larger (in units of the lattice constant) than in chains on a simple cubic lattice or off-lattice chains (measured in units of the LJ distance). The large bond length gives rise to small wave vectors.
(39) Grassberger, P.; Sutter, P.; Schäfer, L. *J. Phys. A: Math. Gen.* **1997**, *30*, 7039. Sutter, P.; Grassberger, P.; Schäfer, L. *Int. J. Mod. Phys.* **1998**, *B12*, 1397.
(40) Debye, P. *Z. Phys.* **1930**, *28*, 138.
(41) Deviations from the plateau in the Kratky plot are also found for other architectures (e.g., rings or star polymers). The structure factor of star polymers and single arms has been calculated by Alessandrini and Carignano[6] by RG calculations and studied experimentally by Willner et al. [Willner, L.; Jucknischke, O.; Richter, D.; Roovers, J.; Zhou, L. L.; Toporowski, P. M.; Fetters, L. J.; Huang, J. S.; Lin, M. Y.; Hadjichristidis, N. *Macromolecules* **1994**, *27*, 3821]. Although the deviations from the Gaussian behavior appear similar the effect is different.

MA991932U